Photoinduced electron-transfer in perylenediimide triphenylamine-based dendrimers: single photon timing and femtosecond transient absorption spectroscopy†‡

Eduard Fron,[a] Roberto Pilot,[a] Gerd Schweitzer,[a] Jianqiang Qu,[b] Andreas Herrmann,[b] Klaus Müllen,[b] Johan Hofkens,[a] Mark Van der Auweraer*[a] and Frans C. De Schryver*[a]

Received 29th November 2007, Accepted 14th February 2008
First published as an Advance Article on the web 13th March 2008
DOI: 10.1039/b718479d

The excited state dynamics of two generations perylenediimide chromophores substituted in the bay area with dendritic branches bearing triphenylamine units as well as those of the respective reference compounds are investigated. Using single photon timing and multi-pulse femtosecond transient absorption experiments a direct proof of a reversible charge transfer occurring from the peripheral triphenylamine to the electron acceptor perylenediimide core is revealed. Femtosecond pump–dump–probe experiments provide evidence for the ground state dynamics by populating excited vibronic levels. It is found by the means of both techniques that the rotational isomerization of the dendritic branches occurs on a time scale that ranges up to 1 ns. This time scale of the isomerization depends on the size of the dendritic arms and is similar both in the ground and excited state.

Introduction

On the basis of their high fluorescence quantum yields and photostability, families of aromatic mono- and di-imide dyes have been used widely as electron acceptors in many fundamental studies of photoinduced electron-transfer including models for photosynthesis,[1–5] solar cells,[6] molecular electronics[7] and dye lasers[8]. The efficient photoinduced charge transfer in a complex structure containing a perylenediimide moiety as acceptor led to the engineering of novel materials with high performance in thin-film organic photovoltaic technology[9].

As a donor unit redox-active triphenylamino (**TPA**) groups, which are extensively used as hole-transport and electron-donor materials,[10,11] were attached into the bay area of the perylenediimide chromophore (**PDI**) *via* dendritic arms. Connecting the two active units with rigid and well defined polyphenylene dendritic arms of different length as spacers allows tuning the donor–acceptor distance. The dendritic branches bearing the **TPA** units at the periphery additionally create a shield around the dye and prohibit aggregation which could influence the photoluminescence properties of the core. It has been pointed out that due to the rotational flexibility of the bay substituents the optical properties of the core chromophore can be affected.[12–14]

In this study the photoinduced formation of a radical ion pair in two dendronized perylenetetracarboxdiimides with 8 and 16 peripheral triphenylamines in toluene is systematically studied. Experimentally, the photoinduced charge-transfer processes in these two molecules embedded in a rigid polymer matrix has been suggested by single molecule experiments.[15–17] Fluctuations in fluorescence decay times related to the forward and reverse charge transfer were reported to be induced on the one hand, by conformational changes in the dendrimer arms (librations) and on the other hand by polymer chain reorientation.

For a direct proof of the radical anion formation femtosecond pump–probe and pump–dump–probe time-resolved transient absorption experiments have been carried out. The results obtained by these techniques were then compared with analogous data obtained from reference compounds of the corresponding generation without **TPA** units. An acronym of the type **PDInN**$_m$ is used in this study to refer to the molecules under investigation. **PDI** denotes the chromophore core of the molecule, $n = 1, 2$, the generation number of the dendritic arms attached to it, and **N**$_m$ the type and the number of triphenylamino group at the rim of the molecules (**N**$_8$, *e.g.*, denoting 8 **TPA** groups). The systems containing no amino groups ($m = 0$) are referred to as **PDIn**. The molecular structures of derivatives of **PDI** bearing polyphenylene dendritic arms in the bay position **PDI1** and **PDI2** and the corresponding systems substituted with **TPA** moieties in first (**PDI1N**$_8$) and second generation (**PDI2N**$_{16}$) are shown in Fig. 1. It should be pointed out that for the **TPA** substituents no different positional isomers are possible.

Experimental

Synthesis and steady state measurements

The synthesis of the derivatives of perylenediimide bearing polyphenylene dendrimers up to the second generation **PDI1** and **PDI2** and the analogous systems substituted with an increasing number of triphenylamine moieties at the periphery **PDI1N**$_8$ and **PDI2N**$_{16}$ was published previously.[11] The electron donor/acceptor capacity of the **TPA**/**PDI** pair is given by the oxidation

[a]*Department of Chemistry and Institute of Nanoscale Physics and Chemistry, Katholieke Universiteit Leuven, Celestijnenlaan 200 F, 3001, Heverlee, Belgium*
[b]*Max-Planck-Institute for Polymer Research, Ackermannstrasse 10, 55128, Mainz, Germany*

† This paper was published as part of the themed issue in honour of Jakob Wirz.

‡ Electronic supplementary information (ESI) available: Fig. 1 SI and Fig. 2 SI. See DOI: 10.1039/b718479d

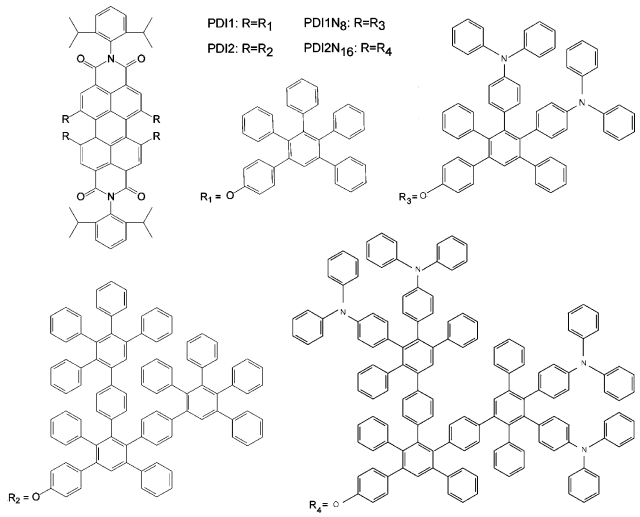

Fig. 1 Molecular structures of **PDI1**, **PDI2**, **PDI1N**$_8$ and **PDI2N**$_{16}$.

(E_{ox}= 0.98 eV *vs.* SCE ref. electrode in CH_3CN)[18] and reduction (E_{red}=−0.43 V *vs.* SCE in DMF + 0.1M Bu_4NPF_6)[19] potential, respectively.

All stationary measurements have been recorded using a fluorimeter (Lambda 40, Perkin Elmer) and a spectrophotometer (Fluorolog, Perkin Elmer). The compounds were investigated in toluene.[20] The optical density at the absorption maximum of all solutions was kept below 0.1 in a 1 cm cuvette. The excitation wavelength was set to 543 nm. The fluorescence quantum yields of the perylenediimide core dendrimers were determined using cresyl violet in ethanol as a reference.[21]

Picosecond fluorescence time-resolved experiments

The fluorescence decay times have been determined by single-photon-timing (SPT) measurements described in detail previously.[22] All measurements have been performed in toluene in a 1 cm optical path length cuvette at an optical density of *ca.* 0.1 at the excitation wavelength of 543 nm. The quality of the fits has been judged by the fit parameters χ^2 (< 1.2), $Z\chi^2$ (< 3) and the Durbin Watson parameter (1.8 < DW < 2.2) as well as by the visual inspection of the residuals and autocorrelation function.[23]

Femtosecond transient absorption measurements

Two femtosecond techniques based on two- and three-beam excitation, namely pump–probe and pump–dump–probe, respectively, were used in the investigation. Both were performed with an amplified femtosecond double OPA laser system which has been described previously,[24] which provides two independently tunable intense pulses used for excitation and one weak pulse used for probing the changes in absorption in a wavelength range between 470 nm and 770 nm. The generation of the probing light was done by focusing an 800 nm beam in a 3 mm sapphire plate to obtain white light in the visible region. The polychromatic detection was done with a CCD Camera (EEV 30, Princeton Instruments) at the first exit of a 30 cm focal length spectrograph (SP300i, Acton Research) whereas the monochromatic detection was performed using a PMT (R1527p, Hamamatsu) placed at the second exit of the spectrograph mounted behind a slit. The pulse duration was 250 fs cross correlation (FWHM). The femtosecond transient absorption experiments were performed at a pump energy density of 2 mJ cm^{-2} pulse^{-1} for both 580 and 645 nm pulses. For the pump–probe experiments the probing was done under magic angle conditions (54.7° relative orientation between the pump and probe polarization planes). In the pump–dump–probe experiments the polarization planes of the two intense laser pulses pump and dump were set to a parallel orientation whereas the probe pulse was polarized under a magic angle configuration relative to the pump pulse polarization plane. The highest value in optical density change observed was still well below the saturation level.

In all experiments the sample was deoxygenated using the consecutive freeze–pump–thaw cycle method. The compounds were dissolved in toluene at a concentration that yielded an absorbance of *ca.* 0.4 per mm at the excitation wavelength of 580 nm. The sample was contained in a quartz cuvette with an optical path length of 1 mm. To improve the signal to noise ratio, every measurement was averaged 15 times at each of the 512 delay positions. The delay position is referred to as the time interval between the arrival of the pump and the probe pulses at the sample position. After each experiment the integrity of the samples has been checked by recording the steady state absorption and emission spectra and comparing them with those obtained before the experiments. No spectral changes suggesting photodegradation were observed. To obtain all different kinetic components, all monochromatic transient absorption traces were globally analyzed over two time windows of 50 and 420 ps. The ns decay times of the components found in SPT experiments were kept fixed during this fit procedure.

Results and discussion

Stationary measurements

The normalized absorption and emission spectra of **PDI1** and **PDI2** are displayed in Fig. 2. The absorption spectra are characterized by a peak (570–580 nm) and a shoulder (530–540 nm) which corresponds to $S_0 \rightarrow S_1$ transition of **PDI** oriented along the long axis. A second peak (440–450 nm) is attributed to the $S_0 \rightarrow S_2$ transition oriented perpendicular to the long axis. With the excitation wavelength used the polyphenylene moieties cannot be excited.[11]

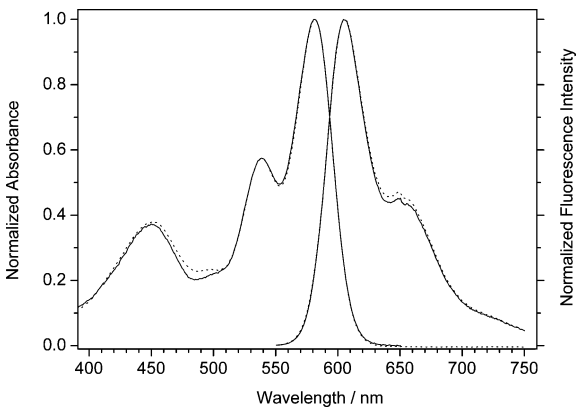

Fig. 2 Normalized steady state absorption and emission spectra (λ_{exc} = 543 nm) of **PDI1** (solid), **PDI2** (dotted) in toluene.

Table 1 Fluorescence quantum yield, absorption and emission maxima of **PDI1**, **PDI2**, **PDI1N$_8$** and **PDI2N$_{16}$** in toluene

Compound	**PDI1**	**PDI2**	**PDI1N$_8$**	**PDI2N$_{16}$**
Fluorescence quantum yield	0.88	0.85	0.14	0.51
Absorption maxima/nm	581	582	581	581
Emission maxima/nm	604	605	603	605

No spectral shift is observed between **PDI1** and **PDI2** neither in absorption nor in fluorescence. The fluorescence quantum yields are high for both **PDI1** and **PDI2** (see Table 1) but decrease slightly in the second generation indicating that additional nonradiative decay channels are being opened.

The enhanced absorption of the $S_0 \rightarrow S_2$ transition observed for the **PDI1** and **PDI2** compared to the phenoxy-substituted **PDI** suggests an increased conjugation with the polyphenylene branches.[25]

The well separated absorption of the **TPA** substituted polyphenylene dendrons allows a selective excitation of the central **PDI** chromophore.[25,26]

The fluorescence quantum yields measured in aerated conditions are compiled in Table 1.

No change in the absorption and emission spectra was observed for **PDI1N$_8$** and **PDI2N$_{16}$** (see Fig. 3) when these are compared to the spectra of **PDI1** and **PDI2**. This indicates that at all times the emission occurs from the locally excited state (LES). A decrease in quantum yield observed for **PDI2N$_{16}$** and more severe in **PDI1N$_8$** while not observed for **PDI2** and **PDI1** indicates a quenching process related to the presence of the amino groups.

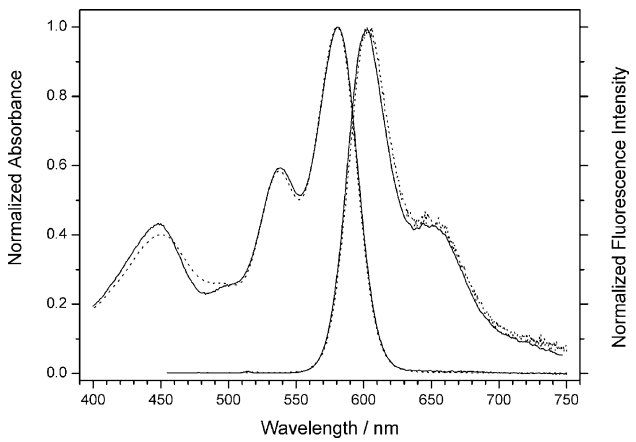

Fig. 3 Normalized absorption and emission spectra (excitation at 543 nm) of **PDI0N$_8$** (solid), **PDI0N$_{16}$** (dotted) in toluene.

Single photon timing experiments

The fluorescence decay times and the corresponding amplitudes obtained from the analysis of the SPT experiments are summarized in Table 2.

The fluorescence decays of **PDI1** and **PDI2** in toluene have to be analyzed as a sum of two exponentials. Besides a slow decaying component with a decay time of $\tau_F = 5.9$ ns ($\tau_F = 5.8$ ns) a fast decaying component with a decay time of $\tau_{conf} = 0.75$ ns ($\tau_{conf} = 1.08$ ns) is recovered for **PDI1** (**PDI2**), respectively. The amplitudes of the latter component have positive values (decay component) at short emission wavelengths and become negative (rise component) towards the red part of the spectrum (Fig. 4). The wavelength dependence of the amplitudes and especially the negative amplitudes at long wavelengths suggests the conversion of a species emitting at shorter wavelengths into a species emitting at longer wavelengths. Assuming that both species have a similar radiative rate constant and molar extinction coefficient at the excitation wavelength the small amplitude of the fast decaying component even at the shortest wavelengths (always $< 20\%$) suggests that the species with the smallest excitation energy is

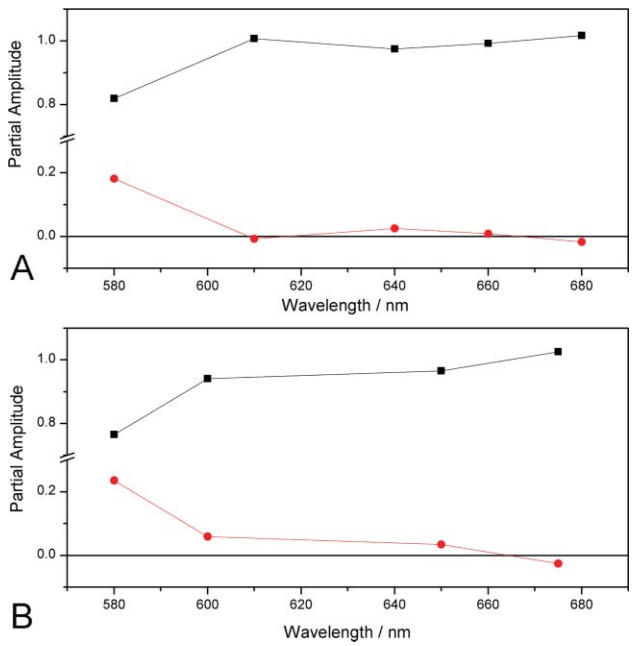

Fig. 4 (A) Wavelength dependence of the partial amplitudes of the decay components found for **PDI1**, $\tau_F = 5.9$ ns (black), $\tau_{conf} = 0.75$ ns (red). (B) Wavelength dependence of the partial amplitudes of the decay components found for **PDI2**, $\tau_F = 5.8$ ns (black), $\tau_{conf} = 1.08$ ns (red); $\lambda_{ex} = 543$ nm.

Table 2 Decay times (in brackets: partial amplitude in %) obtained by SPT measurements ($\lambda_{exc} = 543$ nm, $\lambda_{detect} = 600$ nm)

Compound	Fluorescence τ_F/ns	Fast delayed fluorescence τ_{DF}/ns	Slow delayed fluorescence τ_{DF}/ns	Conformational change τ_{CONF}/ns	Slow CT formation τ_{CTslow}/ns	Fast CT formation τ_{CTfast}/ns
PDI1	5.9[a]	—[b]	—[b]	0.75[a]	—[b]	—[b]
PDI2	5.8[a]	—[b]	—[b]	1.08[a]	—[b]	—[b]
PDI1N$_8$	6.5[c] (9)		22.2 (19)	1.2[c] (10)		0.07 (62)
PDI2N$_{16}$	6.5[c] (65)		12 (6)	1.6[c] (14)		0.14 (15)

[a] For the wavelength dependence of the partial amplitude see Fig. 4. [b] Not found. [c] Mixed value, experimentally/analytically not resolved.

already significantly populated in the ground state and/or that the equilibrium between the two species is only disturbed to a minor extent upon excitation. Considering earlier reports by Würthner *et al.* on bay substituted **PDI**,[13,14] those species could be related to a different orientation of the dendrimer branches. The short decay time is attributed to a reorientation of the dendrimer branches. Hence, in agreement with our observations it will increase with the extension of the size of the phenoxy substituents.

For **PDI1N**$_8$ and **PDI2N**$_{16}$ the fluorescence decays require four exponentials to obtain good fits (see Table 2). The components with decay times slower than 6.5 ns, $\tau_{DFslow} = 22.2$ ns (19%) and $\tau_{DFslow} = 12$ ns (6%), indicate the occurrence of the back electron transfer from the CT state to the LES. While the $\tau_{F/DF} = 6.5$ ns components are attributed to the unquenched **PDI** fluorescence or the delayed fluorescence (*vide infra*), the faster decays $\tau_{CTfast} = 0.07$ ns (62%) and $\tau_{CTslow} = 1.2$ ns (10%) for **PDI1N**$_8$ and $\tau_{CTfast} = 0.14$ ns (15%) and $\tau_{CTslow} = 1.6$ ns (14%) for **PDI2N**$_{16}$ reflect the formation of a CT state or equilibration between a CT state and the LES.[16] It should be pointed out that the extracted decay times are no longer single values but an average over a distribution of decay times. The time components found in the model compounds and attributed to conformational changes are not observed independently since their value ranges overlap with those related to formation of the CT state and all amplitudes are small.

Femtosecond polychromatic transient absorption experiments

Pump–probe experiments. The three dimensional femtosecond transient absorption spectra of **PDI1** and **PDI2** feature a negative band due to a combined effect: ground state depletion (500–600 nm) and stimulated emission (570–670 nm). Simultaneously, a positive band (670–730 nm) is observed and attributed to the absorption of the lowest electronic singlet excited state ($S_1 \rightarrow S_n$). Both bands (see Fig. 5 and Fig. 6) decay simultaneously. All decays have to be analysed as a sum of 4 exponentials. The amplitude of each component is then plotted *versus* wavelength to assist in identifying the corresponding kinetic process. Besides two fast decaying components independently retrieved in the shortest time window (50 ps) for both **PDI1** and **PDI2** and attributed to IVR (the $\tau_{IVR} = 0.5$–2 ps component, wavelength dependent) and vibrational and/or solvent relaxation processes in the electronically excited state (the $\tau_{VR} = 9$–13 ps component, compound dependent) two slower decaying components are observed.

PDI1. For the slower decaying components the analysis of the transient absorption spectra of **PDI1** in toluene (see Fig. 5) reveals a component with a decay time of $\tau_{conf} = 760$ ps and a component with a decay of several ns that could be fixed to $\tau_F = 5.9$ ns. Considering the small amplitude of the 760 ps component and the similarity with the decay time of the component recovered by SPT this component can be attributed to rotational conformational changes of the dendrimer branches.

PDI2. **PDI2** shows decay components of $\tau_F = 5.8$ ns and a $\tau_{conf} = 1070$ ps, the latter is slower than that one for **PDI1** and its amplitude is slightly reduced (see Fig. 6).

The similar SPT and femtosecond experimental data indicate the presence of two different pools of rotational isomers one evolving into the other on a time scale that appears to be related to size of the arms.

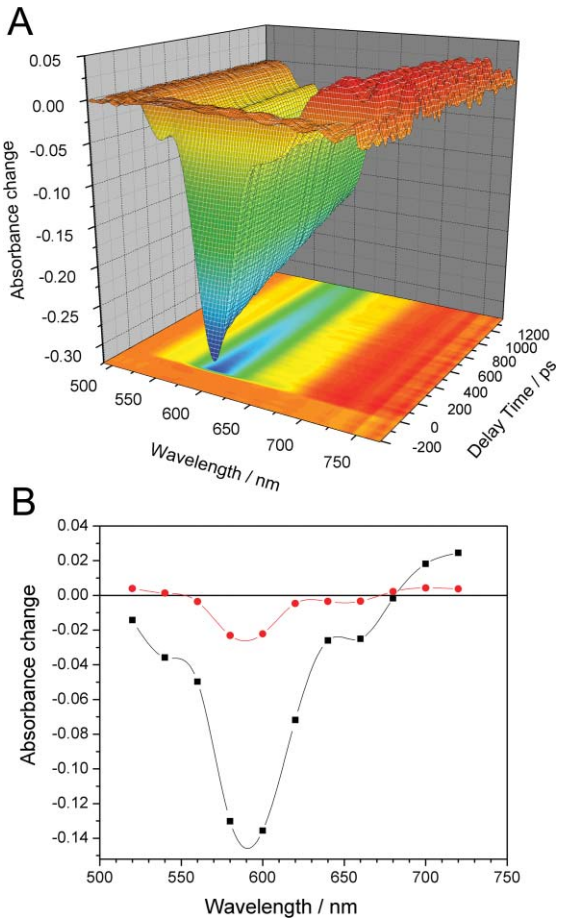

Fig. 5 (A) Three-dimensional plot of the transient absorption spectra of **PDI1** in toluene. (B) Wavelength dependence of the partial amplitudes: $\tau_F = 5.9$ ns (black), $\tau_{conf} = 760$ ps (red).

PDI1N$_8$. The time resolved transient absorption spectra of **PDI1N**$_8$ recorded in the 420 ps time window is displayed in Fig. 7A The negative band (600–670 nm) is attributed to the ground state depletion and stimulated emission from the LES. The positive band (670–770 nm) appears clearly wider and more intense compared to the corresponding transient of **PDI1**. The difference in shape and intensity observed for **PDI1N**$_8$ could be linked to the presence of a **PDI** radical anion absorption band in agreement with literature.[27,28] Considering the overlap of the two bands and their similar extinction coefficients, the broadening of the positive signal and the rise (760 nm) of the absorption observed in the first 100 ps suggests the formation of the radical anion. To get better evidence for the photoinduced charge transfer process a global kinetic analysis involving 26 wavelengths has been carried out. A plot of a few kinetic traces recorded in the 100 ps time window and the corresponding fits are shown in Fig. 1 SI of the electronic supplementary information, ESI.‡ Besides IVR and VR two time constants of $\tau_{CTfast} = 70$ ps and 5.5 ns were necessary to obtain good fits. Their partial amplitudes have then been plotted against the wavelength giving support to identification of each process (see Fig. 7(B)). Furthermore the spectral behaviour of the longest decay time 5.5 ns bears a resemblance to the one obtained for **PDI1**. This component can be considered as a combination of the $\tau_{CTslow} = 1.2$ ns, $\tau_{DFfast} = 6.5$ ns and $\tau_{DFslow} = 20$ ns decay times

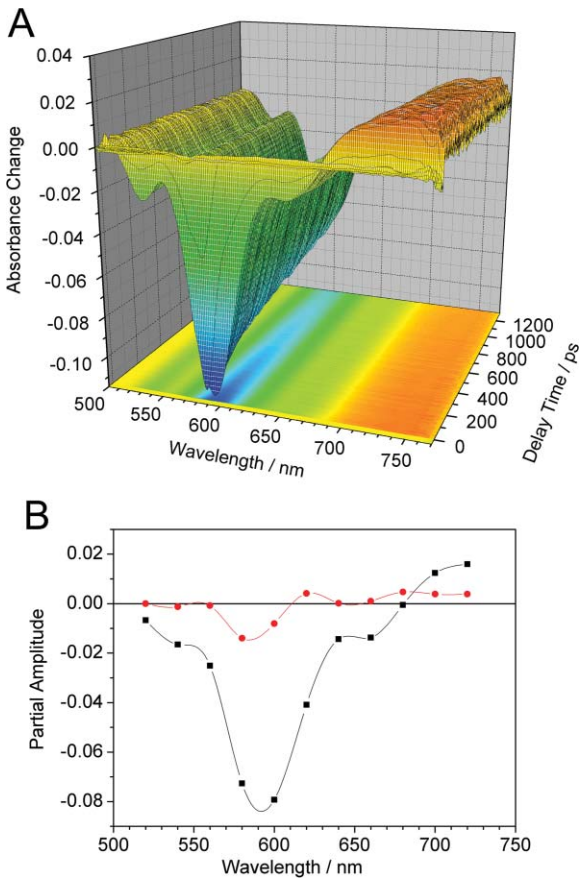

Fig. 6 (A) Three-dimensional plot of the transient absorption spectra of **PDI2** in toluene. (B) Wavelength dependence of the partial amplitudes: $\tau_F = 5.7$ ns (black), $\tau_{conf} = 1070$ ps (red).

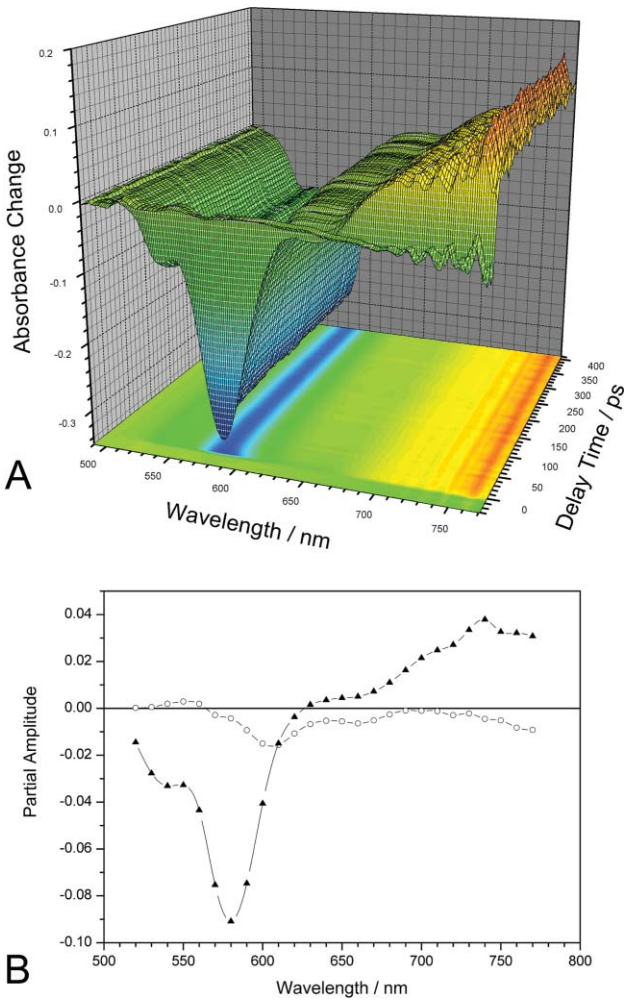

Fig. 7 (A) Three-dimensional display of the transient absorption spectra of **PDI1N**$_8$ in toluene recorded in a 420 ps time window. (B) Wavelength dependence of the partial amplitudes of the decay times obtained by global analysis: $\tau_{CTfast} = 70$ ps (○) and 5.5 ns (▲).

found in SPT and not discriminated here by the fit analysis. As compared to the model compound a difference is observed in the wavelength region (600–670 nm) where stimulated emission is more outspoken for **PDI1**.

The 70 ps component which is also found in the SPT experiments but that is not present in **PDI1** shows negative amplitudes in the region 600–770 nm with a small contribution of induced emission in the related region. Although the CT and S_1–S_n absorption bands overlap to a large extent the CT absorption is more pronounced in the red region. The negative signal beyond 700 nm corresponds to the rise of the photoinduced CT state absorption when ε_{A^-} (extinction coefficient for the anion absorption) is larger than $\varepsilon_{S_1 \rightarrow S_n}$ (extinction coefficient for the excited state absorption of the locally excited state). Therefore the 70 ps kinetic component can be attributed to the formation of a radical anion. A back charge transfer process repopulates the LES and the fluorescence is found to occur exclusively from the S_1 state. This is also supported by the stationary emission spectrum while the decrease of the quantum yield indicates the presence of new nonradiative pathways within the CT state.

PDI2N$_{16}$. The rise of the **PDI** radical anion band is also demonstrated by means of femtosecond transient absorption measurements for **PDI2N**$_{16}$. The respective three-dimensional time resolved spectra recorded in a 1400 ps time window are displayed in Fig. 8(A). As discussed for **PDI2** (*vide supra*), one can again observe the ground state depletion and stimulated emission band as a negative absorption with a minimum centred at 580 nm. Similar to **PDI1N**$_8$ the radical anion absorption of the **PDI** and the S_1–S_n excited state absorption bands overlap largely thus hindering the observation of the radical anion signal. A plot of a few kinetic traces with the corresponding fits recorded in 1400 ps time interval is shown in Fig. 2 SI.‡ In addition to the IVR and VR components, two kinetic components of $\tau_{CTfast} = 140$ ps and 5.7 ns were retrieved by means of the kinetic analysis, the wavelength dependence of their amplitudes is plotted in Fig. 8(B). The 5.7 ns decay time could be related to a superposition of the $\tau_{CTslow} = 1.6$ ns, $\tau_{DFfast} = 6.5$ ns and $\tau_{DFslow} = 12$ ns components retrieved by SPT experiments and not resolved here further.

In the analysis of the ensemble experimental data, the retrieved time constants for charge transfer are an average over different conformers present in the sample. The long component of 5.7 ns with large amplitude at shorter wavelengths resembling a combination of ground state recovery, stimulated emission and at longer wavelengths excited state absorption can be partially attributed to the delayed fluorescence of the LES as well as to molecules not involved in charge transfer. It has a similar spectral shape as the long component found for **PDI2** and its large amplitude

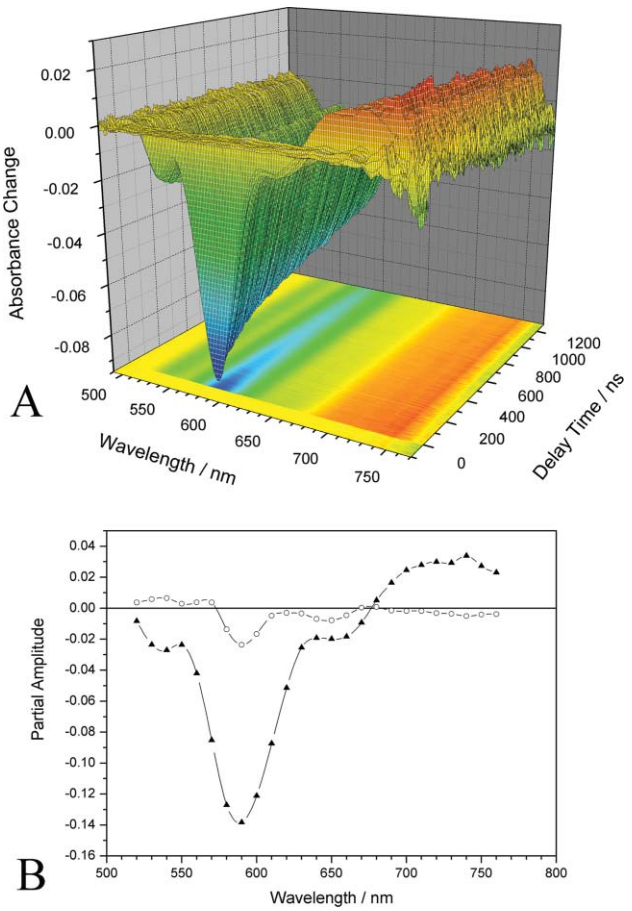

Fig. 8 (A) Three-dimensional display of the transient absorption spectra of **PDI2N**$_{16}$ in toluene recorded in a 1400 ps time window. (B) Wavelength dependence of the partial amplitudes of the decay components obtained by global analysis: τ_{CTfast} = 140 ps (○) and 5.7 ns (▲).

indicates that this fraction is very important (65%) as recovered in SPT experiments. The other component of 140 ps also revealed in the SPT measurements but not found in **PDI2** has a very similar spectral shape as the 70 ps component found for **PDI1N**$_8$. Between 670 and 760 nm the molar extinction coefficients of the $S_1 \rightarrow S_n$ absorption and the absorption of the species formed nearly cancel leading to very small negative amplitudes. The 140 ps component can therefore be attributed to the formation of **PDI** radical anion absorption. The slower charge transfer time constants as compared to those of **PDI1N**$_8$ can be explained by the larger average distance between the amino groups and the central **PDI** chromophore. The mechanism for the charge transfer and the role of the polyphenylene branches in this process was reported earlier.[16]

Pump–dump–probe experiments. An elegant way to discriminate between processes that might occur either in the excited or the ground state is to make use of the femtosecond pump–dump–probe scheme in transient absorption experiments. Using this general method, the molecular system is initially excited to the S_1 state and then using lower resonant energy pulses, the higher vibronic levels of the S_0 state are populated *via* stimulated emission. In order to do that a femtosecond excitation pulse at 580 nm is used to excite the **PDI** core out of the thermally populated S_0 state into S_1 while a second pulse tuned to 645 nm and delayed by 4 ps is used to transfer population out of this state by stimulated emission (see Fig. 9). The delay of 4 ps was chosen to allow the IVR processes (with large amplitude) in the excited state to complete while the VR processes are still at the beginning. In this way the preparation of vibrationally excited **PDI1N**$_8$ molecules on the S_0 surface is achieved. The energy difference between the pump and the dump pulses indicates the mean vibrational energies for the prepared non-equilibrated S_0 state. A third weak pulse probes the absorption changes similar to the technique used in the pump–probe experiments. By monitoring the kinetics of the ground (580 nm) and the excited state (610 nm) with and without the application of the dump pulse the dynamic relaxation processes occurring in the ground and excited state can be studied.

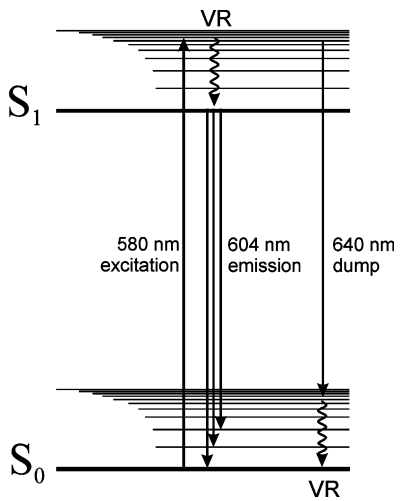

Fig. 9 Schematic energy level diagram of **PDI1N**$_8$ showing the pump and dump pulses with the respective wavelengths.

Fig. 10(A) displays the transient absorption spectra of **PDI1N**$_8$ before (4 ps) and after (5 ps) the action of the dump pulse. It is observed that the changes in the spectra occur only in the wavelength regions of the stimulated emission and excited state absorption, whereas the transient signal corresponding to the ground state recovery remains almost unchanged. The intense decrease of these two signals indicates an important depopulation of the S_1 state induced by the dump pulse prior to the occurrence of the VR process in the excited state. The population is transferred to the upper vibronic levels of the S_0 state, where it concurrently relaxes to an equilibrium distribution.

The decay traces recorded at 610 nm wavelength with and without the contribution of the dump pulse and the corresponding fits are plotted in Fig. 10(B). When only the excitation pulse is present the VR process is found to occur with a time constant of τ_{VRES} = 10.8 ps (black trace in Fig. 10(B)) with a similar kinetic as presented earlier. Upon the action of the dump pulse a component of $\tau_{VR\ Equilibration}$ = 18 ps is retrieved from the kinetic analysis instead of the 10.8 ps (blue trace in Fig. 10(B)). Since this stimulated emission signal (610 nm) monitors the remainder of the thermally non equilibrated population of the S_1 state this slower component could be regarded as the time necessary for this fraction of molecules to relax to the bottom of the S_1 state. This would also explain the small rise observed after the dump pulse in Fig. 10(B). Another explanation for this 18 ps component (and the

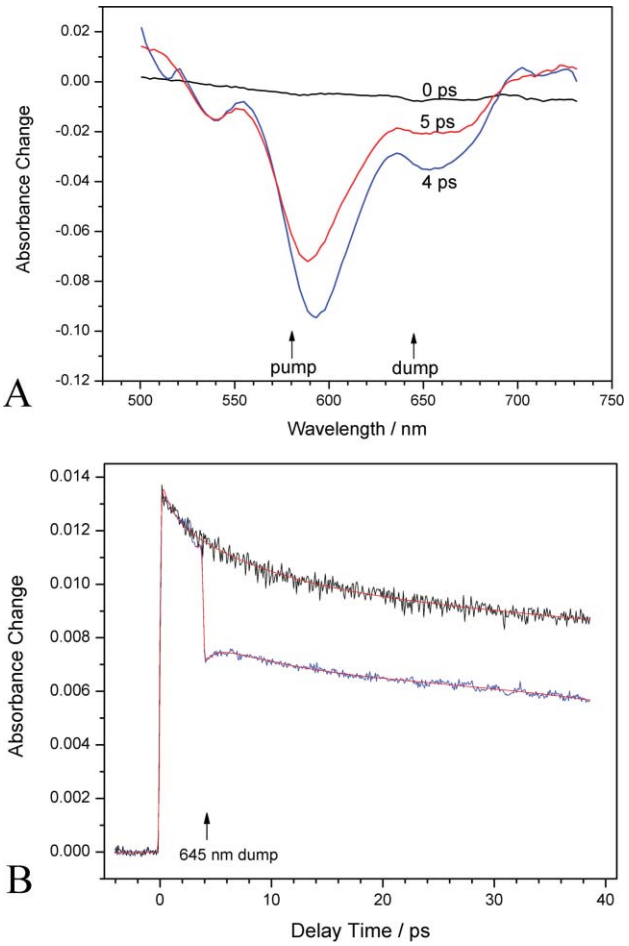

Fig. 10 (A) Femtosecond transient absorption 2D spectra of **PDI1N**$_8$ at 0 ps (black), 4 ps (blue) and 5 ps (red) (645 nm dump wavelength, 4 ps dump delay). (B) Decay traces and the corresponding fits obtained with pump–probe (black) and pump–dump–probe (blue) geometry recorded at 610 nm wavelength (PMT detection).

rise after the 645 nm pulse in Fig. 10(B)) could be repopulation of the S_1 state following $S_1 \rightarrow S_n$ excitation by the 645 nm pulse followed by relaxation to the S_1 state.

The analysis of the signal corresponding to the ground state recovery (580 nm detection wavelength) reveals information about the relaxation dynamics of that state. The kinetic analysis of this decay trace (Fig. 11) revealed a component of $\tau_{VRGS} = 11.5$ ps which is, within experimental errors, the value of the VR time constant found for the excited state in the absence of the dump pulse.

In addition, the $\tau_{CTfast} = 70$ ps component (detected in the S_1 state) has a smaller amplitude compared to the analogous one shown in Fig. 7(B), which is explained by a reduced creation of the CT state. The formation of the CT state is partially inhibited by the effect of the dump pulse which transfers a significant part of the S_1 population directly to the ground state.

Conclusions

Femtosecond transient absorption data presented in this study provided clear spectroscopic evidence of a charge transfer in the first and second generation of a polyphenylene dendrimer containing several triphenylamine donors and a perylenediimide

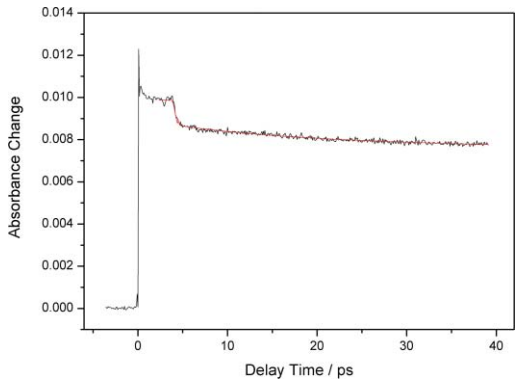

Fig. 11 Decay traces and the corresponding fits obtained with pump—dump–probe geometry recorded at 580 nm wavelength (PMT detection).

acceptor. The results were compared to the data obtained from the corresponding model compounds where no charge transfer was observed. The investigation of the model compounds also provided information on the rotational reorientation of dendrimer branches of the bay substituted polyphenylene branches taking place with time constants that depend on their size.

The electron transfer is found to be reversible with the emission occurring at all times from the lowest single excited state. In **PDI2N**$_{16}$ the charge transfer occurs at a lower rate due to a larger donor–acceptor separation. Taking advantage of the pump–dump–probe technique the investigation of the ground state reveals a vibrational relaxation that is similar to the one observed in the excited state. Furthermore, in these experiments an important fraction of the population found in the singlet excited state is depleted to the ground state by stimulated emission prohibiting the formation of the charge transfer state.

Acknowledgements

Support from the FWO, the Flemish Ministry of Education (GOA 2006/2), the IWT through ZWAP 04/007 and the BMBF, the Federal Science Policy of Belgium (IAP-VI-27) is acknowledged. A Max Planck research award is also acknowledged. The authors thank Prof. F. Würthner for sharing unpublished information and fruitful discussions.

References

1 S. R. Greenfield, W. A. Svec, D. Gosztola and M. R. Wasielewski, Multistep Photochemical Charge Separation in Rod-like Molecules Based on Aromatic Imides and Diimides, *J. Am. Chem. Soc.*, 1996, **118**, 6767–6777.
2 G. P. Wiederrecht, M. P. Niemczyk, W. A. Svec and M. R. Wasielewski, Ultrafast Photoinduced Electron Transfer in a Chlorophyll-Based Triad: Vibrationally Hot Ion Pair Intermediates and Dynamic Solvent Effects, *J. Am. Chem. Soc.*, 1996, **118**, 81–88.
3 A. Osuka, N. Mataga and T. Okada, A chemical approach towards the photosynthetic reaction center, *Pure Appl. Chem.*, 1997, **69**, 797–802.
4 A. Osuka, S. Marumo, T. Okada, S. Taniguchi, N. Mataga, T. Ohno, K. Nozaki, I. Yamazaki and Y. Nishimura, A Full Charge Separation over the Two Same Chromophores in a Photosynthetic Tetrad, *J. Photosci.*, 1997, **4**, 113–119.
5 H. Levanon, T. Galili, A. Regev, G. P. Wiederrecht, W. A. Svec and M. R. Wasielewski, Determination of the Energy Levels of Radical Pair States in Photosynthetic Models Oriented in Liquid Crystals with Time-Resolved Electron Paramagnetic Resonance, *J. Am. Chem. Soc.*, 1998, **120**, 6366–6373.

6 M. A. Angadi, D. Gosztola and M. R. Wasielewski, Characterization Of Photovoltaic Cells Using Poly (Phenylenevinylene) Doped With Perylenediimide Electron Acceptors, *J. Appl. Phys.*, 1998, **83**, 6187–6189.
7 M. P. Debreczeny, W. A. Svec, E. M. Marsh and M. R. Wasielewski, Femtosecond Optical Control of Charge Shift within Electron Donor–Acceptor Arrays: An Approach to Molecular Switches, *J. Am. Chem. Soc.*, 1996, **118**, 8174–8175.
8 M. Sadrai, L. Hadel, R. R. Saures, S. Husain, K. Krogh-Jespersen, J. D. Westbrook and G. R. Bird, Lasing action in a family of perylene derivatives: singlet absorption and emission spectra, triplet absorption and oxygen quenching constants, and molecular mechanics and semiempirical molecular orbital calculations, *J. Phys. Chem.*, 1992, **96**, 7988–7996.
9 L. Schmidt-Mende, A. Fechtenkötter, K. Müllen, E. Moons, R. H. Friend and J. D. MacKenzie, Self-organized Discotic Liquid Crystals for High-Efficiency Organic Photovoltaics, *Science*, 2001, **293**, 1119–1122.
10 U. Bach, K. de Cloedt, H. Spreitzer and M. Graetzel, Characterization of Hole Transport In A New Class Of Spiro-Linked Oligotriphenylamine Compounds, *Adv. Mater.*, 2000, **12**, 1060–1063.
11 J. Q. Qu, N. G. Pschirer, D. J. Liu, A. Stefan, F. C. De Schryver and K. Müllen, Dendronized Perylenetetracarboxdiimides With Peripheral Triphenylamines for Intramolecular Energy and Electron Transfer, *Chem.–Eur. J.*, 2004, **10**, 528–537.
12 C. Hippius, I. H. M. van Stokkum, E. Zangrando, R. M. Williams and F. Würthner, Excited State Interactions in Calix[4]arene-Perylene Bisimide Dye Conjugates: Global and Target Analysis of Supramolecular Building Blocks, *J. Phys. Chem. C*, 2007, **111**, 13988–13996.
13 E. Lang, R. Hildner, H. Engelke, P. Osswald, F. Würthner and J. Kohler, Comparison of the Photophysical Parameters for Three Perylene Bisimide Derivatives by Single-molecule Spectroscopy, *ChemPhysChem*, 2007, **8**, 1487–1496.
14 F. Würthner, Bay-substituted perylene bisimides: Twisted fluorophores for supramolecular chemistry, *Pure Appl. Chem.*, 2006, **78**, 2341–2349.
15 M. Cotlet, S. Masuo, M. Lor, E. Fron, M. Van, der Auweraer, K. Müllen, J. Hofkens and Frans C. De, Schryver, Probing the influence of O_2 on photoinduced reversible electron transfer in perylenediimide-tryphenylamine-based dendrimers by single-molecule spectroscopy, *Angew. Chem.*, 2004, **116**, 6242–6246.
16 M. Cotlet, S. Masuo, G. Luo, J. Hofkens, M. Van der Auweraer, J. Verhoeven, K. Müllen, X. Sunney Xie and Frans C. De Schryver, Probing conformational dynamics in single donor–acceptor synthetic molecules by means of photoinduced reversible electron transfer, *Proc. Natl. Acad. Sci. USA*, 2004, **101**, 14343–14348.
17 R. Gronheid, A. Stefan, M. Cotlet, J. Hofkens, J. Qu, K. Müllen, M. Van der Auweraer, J. W. Verhoeven and Frans C. De Schryver, Reversible Intramolecular Electron Transfer At The Single-Molecule Level, *Angew. Chem., Int. Ed.*, 2003, **42**, 4209–4214.
18 W. N. Sisk, K.-S. Kang, M. Y. A. Raja and F. Farahi, Matrix And Donor/Acceptor Dependence of Polymer Dispersed Pyrromethene Dye Photoconductivity, *I. J. Optoelectr.*, 1995, **10**, 95–103.
19 D. Gosztola, M. P. Niemczyk, W. A. Svec, A. S. Lukas and M. R. Wasielewski, Excited Doublet States of Electrochemically Generated Aromatic Imide and Diimide Radical Anions, *J. Phys. Chem. A*, 2000, **104**, 6545–6551.
20 *CRC Handbook of Physics and Chemistry*, ed. D. R. LideCRC Press, Boca Raton, FL, 73rd edn, 1992.
21 J. Olmsted, Calorimetric Determinations of Absolute Fluorescence Quantum Yields, *J. Phys. Chem.*, 1979, **83**, 2581–2584.
22 M. Maus, E. Rousseau, M. Cotlet, G. Schweitzer, J. Hofkens, M. Van der Auweraer and F. C. De Schryver, New Picosecond Laser System For Easy Tunability Over The Whole Ultraviolet/Visible/Near Infrared Wavelength Range Based on Flexible Harmonic Generation And Optical Parametric Oscillation, *Rev. Sci. Instrum.*, 2001, **72**, 36–40.
23 D. V. O'Connor and D. Philips, *Time-Correlated Single Photon Counting*, Academic Press, London, 1984.
24 G. Schweitzer, L. Xu, B. Craig and F. C. De Schryver, A double OPA femtosecond laser system for transient absorption spectroscopy, *Opt. Commun.*, 1997, **142**, 283–288.
25 D. Liu, S. De. Feyter, M. Cotlet, A. Stefan, U. Wiesler, A. Herrmann, D. Grebel-Koehler, J. Qu, K. Müllen and F. C. De Schryver, Fluorescence and intramolecular energy transfer in polyphenylene dendrimers, *Macromolecules*, 2003, **36**, 5918–5925.
26 W. Verbouwe, L. Viaene, M. Van der Auweraer, F. C. De Schryver, H. Masuhara, R. Pansu and J. Faure, Photoinduced Intramolecular Charge Transfer in Diphenylamino-Substituted Triphenylbenzene, Biphenyl, and Fluorene, *J. Phys. Chem. A*, 1997, **101**, 8157–8165.
27 D. Gosztola, M. P. Niemczyk, W. A. Svec, A. S. Lukas and M. R. Wasielewski, Excited Doublet States of Electrochemically Generated Aromatic Imide and Diimide Radical Anions, *J. Phys. Chem. A*, 2000, **104**, 6545–6551.
28 C. Hippius, I. H. M. van Stokkum, E. Zangrando, R. M. Williams and F. Würthner, Excited State Interactions in Calix[4]arene-Perylene Bisimide Dye Conjugates: Global and Target Analysis of Supramolecular Building Blocks, *J. Phys. Chem. C*, 2007, **111**, 13988–13996.

